Analysis of Factors Affecting Railway Embankment Settlement due to Liquefaction Using 1-g Shaking Table Model Tests

Ik-Soo Ha
Kyungnam University
I-Tae Oh
Kyungnam University
MINTAEK YOO (thezes03@krri.re.kr)
Korea Railroad Research Institute https://orcid.org/0000-0003-1621-6888

Research Article

Keywords: Shaking table test, Non-liquefiable layer thickness, Railway embankment, Liquefaction, Settlement

Posted Date: March 8th, 2022

DOI: https://doi.org/10.21203/rs.3.rs-1417342/v1

Abstract

Herein, 1-g shaking table tests were performed under test by changing the embankment height and non-liquefiable layer thickness below the embankment for the same input seismic load. Accelerometers, pore water pressure transducers, and linear variable differential transformers were embedded inside the foundation ground or installed on the embankment surface to measure their responses to shaking. The testing procedure for analyzing the behavior of a two-dimensional embankment-ground system and well-documented experimental data are presented. The results show that the settlement of the railway embankment placed on the liquefiable sand ground due to ground liquefaction is greatly affected by the embankment height and non-liquefaction layer thickness, which determine the degree of liquefaction and lateral flow of the foundation ground. The embankment settlement increased with the embankment height due to the liquefaction of the ground and increased by twice the settlement of the ground without embankment when the embankment height was approximately 20% of the total liquefiable sand layer. Moreover, the settlement was reduced by over 20% compared to that without a layer when the layer thickness was 50% of the embankment height. Furthermore, the settlement decreased to a negligible level when it was approximately 1.4 times the height of the embankment.

1. Introduction

Embankments, including river dikes, road embankments, and railway embankments, have been frequently damaged during past major earthquakes in the last decades (Matsuo, 1996; Nozawa et al., 2019). Previous case studies have shown that such embankment damage is dangerous when the underlying saturated cohesionless soils liquefy (Koga et al., 1990). The liquefaction of foundation soils resulted in large deformations or failures of embankments (Park et al., 2000).

Many railroad embankments were seriously damaged to accommodate large settlements during the 1964 Niigata earthquake (Ohki et al., 2004). These settlements were mainly caused by the liquefaction of subsoil, which was affected by the degree of liquefaction and the continued seismic motion, as reported by Sawada et al. (Sawada et al., 2003; Ohki et al., 2004; Ohki et al., 2013). Even a small settlement of the embankment may endanger the safety of train running. Therefore, it is necessary to estimate the settlement of the railroad embankment due to the liquefaction of the foundation soil.

Previous studies have been conducted to estimate the settlement of liquefiable ground due to liquefaction and evaluate the damage caused by liquefaction of the liquefiable ground using the liquefaction potential index (LPI) (Iwasaki et al., 1978; Tokimatsu et al., 1987; Ishihara et al., 1992). However, these studies only suggest solutions to typical one-dimensional problems. In addition, it is impossible to calculate the settlement or evaluate the damage considering two-dimensional or three-dimensional interactions with the upper structures, such as embankments, due to the lack of elaborate experimental data and the complexity of real problems compared to one-dimensional problems. In this regard, it is essential to acquire well-documented experimental data to understand the settlement

behavior because of the two-dimensional interaction between the embankment and the liquefiable soil foundation.

Koga et al. performed a 1-g shaking table test for the analysis of the seismic behavior of the soil embankment placed on a liquefiable soil foundation and presented the research results (Koga et al., 1990). In the test, the effects of input acceleration characteristics such as the wave form, frequency content, and duration time on the settlement of the embankment crest due to the underlying ground were examined for embankments with the same dimensions. Similarly, Park et al. conducted a 1-g shaking table test on gravel embankments of the same dimension and analyzed the effect of applying various countermeasures to minimize the settlement of the embankment crest caused by the liquefaction of the foundation ground (Park et al., 2000). Ohki et al. evaluated the settlement of the embankment according to the degree of liquefaction of subsoil and the duration of the input seismic load using a 1-g shaking table test (Ohki et al., 2004). Based on the test results, it was shown that the embankment settlement was mainly caused by the lateral flow and vertical consolidation of the liquefied subsoil, and it is most effective to restrict the lateral flow of the liquefied subsoil in order to suppress this settlement of the embankment. As the aforementioned studies regarding the 1-g shaking table test on the embankment-foundation system have the same embankment dimensions on the homogeneous liquefiable subsoil, the results are limited in analyzing the behavior of the two-dimensional embankment–ground system based on the change in the embankment height and the change in the stratum composition of the ground under the embankment.

The embankment settlement due to lateral flow is caused by the difference between the changed ground strength based on the changed liquefaction degree of the subsoil below the embankment and the strength in the adjacent free-field ground. Therefore, intuitive model tests are necessary because the influencing factors may be related to the embankment height. This in turn is related to the influence range of the overburden of the embankment and the thickness of the non-liquefiable superficial layer directly below the embankment, which can be the starting point of the lateral flow.

In this study, 1-g shaking table tests were performed on a total of seven cases with test conditions in which the embankment height and the non-liquefiable layer thickness below the embankment were changed for the same input seismic load conditions. During the test, accelerometers, pore water pressure transducers, and linear variable differential transformers (LVDTs) were embedded inside the foundation ground or installed on the surface of the embankment to measure their responses to shaking. The procedure and method for simulating these condition changes with the 1-g shaking table model test is presented in detail. Based on the analysis of the response records, the degree of liquefaction and lateral flow of the foundation ground under the embankment were evaluated, and the qualitative or relative quantitative effects of the embankment height and the non-liquefiable layer thickness on the settlement at the embankment crest were analyzed and presented. Compared to levees, railway embankments are less prone to liquefaction within the embankment. Moreover, the settlement of the embankment itself is relatively small although there is a change in the shape in response to the lateral flow caused by the liquefaction of the subsoil. Considering this point, in this study, the subject embankment was limited to a

railway embankment constructed with well-compacted ballast to exclude the settlement characteristics of the embankment as much as possible and focus on the settlement characteristics of the foundation subsoil due to liquefaction, which is the scope of the study. The model embankment was constructed using gravel to minimize self-settlement and capillary rise.

2. 1-g Shaking Table Model Test Program

2.1 Models

The models were constructed in a rigid Plexiglas container with a length of 2.0 m, a width of 0.5 m, and a height of 0.7 m. Silica sand, whose index properties are listed in Table 1, was used as the liquefiable sand ground in the model. The railway embankment was built using an angular gravel with a size of 1–2 cm with 1:1.8 slopes. The unit weight of the embankment was set to 19.6 kN/□ to adjust the overburden load based on the height and suppress the settlement of the embankment.

Figure 1 shows the seven different test cases that were conducted. In Cases 3 and 4, an additional test was performed to confirm the reproducibility of the same cross-sectional condition (case). As a result, a total of nine tests were performed. Cases 1 to 4 analyze the settlement behavior of the embankment based on the change in the embankment height H. These tests were carried out on a liquefiable sand ground with a thickness of 50 cm but with different gravel embankment heights of 0, 5, 10, and 15 cm. On the other hand,

Cases, 5, 6, and 7 analyze the settlement behavior of the embankment based on the change in the non-liquefiable layer thickness H1. These tests were performed with an embankment height of 10 cm but with different non-liquefiable layer thicknesses of 0, 4.5, 10.5, and 13.5 cm. A railway embankment that was 40 times as large as the model was implemented as the prototype embankment to determine the dimensions of the model in this study. In addition, the height of this prototype embankment was in the range of 2–6 m in South Korea. In addition, considering that the liquefaction evaluation is usually performed within a depth of 20 m, the thickness of the liquefiable sand layer in the model was set to 50 cm, which is 1/40 of 20 m. The embankment height in the model was set to 5, 10, and 15 cm, which were reduced to 1/40 corresponding to 2, 4, and 6 m of the prototype, respectively. However, in a 1-g shaking table test of the reduced scale model, the similitude rule in terms of the stress-strain for a prototype cannot be satisfied because the stress-strain behavior of soil is stress-dependent. Therefore, the model tests presented here must be considered as “small prototype tests.” Furthermore, this study can provide the results of the qualitative evaluation or relative quantitative evaluation of parameters based on the change in the parameters to be reviewed (Sasaki et al., 1983; Iwasaki, 1986; Koga et al., 1990).

2.2 Instrumentation

Three types of sensors, including 11 pore water pressure transducers, 13 accelerometers, and two LVDTs, were embedded inside and at the surface of each model to measure their responses to shaking. Figure 2 shows the instrumentation locations. In particular, the instrument number shown in Fig. 2 indicates a

representative instrument and its location. The response result is presented as a time history in the subsequent section, as shown in Figs. 6 and 9.

Piezometers were used to measure the excess pore water pressure in soils. The piezometer has a diameter of 1.2 cm and a length of 1.1 cm, which is small enough not to affect the test results. They were attached to a vertical steel rod to maintain a position during shaking, as shown in Fig. 3(a). Moreover, accelerometers were used to measure the ground accelerations and were attached to the cap-type acrylic plate to move together with the soil during shaking, as shown in Fig. 3(b). An LVDT was used to measure the embankment settlement or the ground surface settlement. Furthermore, Fig. 3(c) shows that the extension rod tip of the LVDT was attached to the small thin plates placed on the embankment top or the surface of the ground.

2.3 Excitation

Figure 4 shows the input acceleration measured at the bottom of the soil box during the experiments. The input acceleration was a sinusoidal wave of 5 Hz. Based on the results of the pretest for Case 1 (Fig. 1), the maximum main input acceleration was 0.2 g, and the duration time was 5 s to generate liquefaction over the entire height of the model. The level of acceleration was increased from 0.03 to 0.2 g in 1.5 s and decreased in the reverse manner after the main excitation.

2.4 Test Setup for Evaluating the Effect of the Embankment Height

In the case of the embankment placed on the ground made of liquefiable sand, tests were conducted to examine the effect of the embankment height on the settlement behavior due to liquefaction of the subsoil. Figure 1 shows the test conditions corresponding to Cases 1–4.

Most 1-g shaking table tests are performed under atmospheric pressure. Therefore, the model ground has to be made very loose if the model soil is to be liquefied under a low confining pressure in the model ground. Loose sand ground can be prepared using the water sedimentation method. Here, the liquefiable loose sand ground is formed using water by pouring the sand through a 1-mm sieve to reduce the dropping velocity and maintain it as loose as possible. The water table elevation coincided with that of the ground surface.

For Case 1, the submerged unit weight for each depth of the liquefiable sand ground was measured during the preliminary test. A sample can be placed every 10 cm from the bottom of the box when preparing liquefiable subsoil ground. In addition, the ground composition was stopped, the sample was removed, and the weight, volume, and water content were measured to calculate the unit weight when the ground composition was made up to the top of the sample using the water sedimentation method. This process was repeated every 10 cm of ground composition. Considering the excess pore water pressure, the measured submerged unit weight was compared with that obtained by the inverse calculation, as shown in Fig. 7(a). In addition, the measurement depth during liquefaction is shown as a test result for Case 1. The comparison confirmed that the two values were similar. Although the measured submerged

unit weight showed an insignificant difference by depth, it was estimated to be approximately 8.8 kN/□ on average and approximately 25% in relative density. It could be assumed that the saturation degree of the subsoil was approximately 98% based on the void ratio that was calculated by the dry density (0.81), the average water content (0.3), and the specific gravity (2.65).

Cases 2 to 4 are cross-sections with embankments with heights of 5, 10, and 15 cm, respectively, on the foundation ground under the cross-section of Case 1 without an embankment (H = 0 cm). Geotextiles were laid on the surface where the embankment was to be placed to prevent the disturbance of the ground surface and the gravel material (i.e., embankment material) from penetrating into the lower sand layer at the initial stage of construction when the embankment was built on a soft and sensitive liquefiable sand foundation. The embankment was completed by stacking gravel to the target height and on the laid fibers.

All tests were conducted with excitation approximately 15 h after completing the test section.

2.5 Test Setup for Evaluating the Effect of the Non-liquefiable Layer Thickness

Tests were conducted to examine the effect of the non-liquefiable layer thickness of the foundation ground of the embankment with a constant height on the settlement behavior of the embankment due to subsoil liquefaction. Figure 1 shows the test conditions corresponding to Cases 3, 5, 6, and 7.

In this study, the non-liquefiable layer thickness refers to the depth from the ground surface of the foundation to the bottom of the layer under the condition that liquefaction cannot occur, and it is denoted as H1. In this shaking table model test, the non-liquefiable layer corresponds to a sandy ground of medium density or higher located above the groundwater level. This layer is formed by dewatering the foundation ground to the target depth under Case 1 conditions, thereby inducing unsaturated conditions and density-increase conditions. The change in the groundwater level in the liquefiable sand model ground was confirmed using a piezometer installed on the lower side of the soil box.

Figure 5 shows the schematic of the procedure for forming H1 in this test. This procedure is as follows:

1. Total liquefiable foundation ground composition (same as Case 1).
2. A perforated steel pipe is installed and dewatered after excavating the location that does not interfere with the installation of the embankment and burial of instruments to create a non-liquefiable layer. Dewatering is performed to ensure that the water level is deeper than the target water level in consideration of the water level rise due to the installation of the embankment.
3. Build embankments and stabilize the ground for at least 15 h.
4. Check the final groundwater level from the piezometer and determine the depth to the groundwater level as the non-liquefiable layer depth (depth from the surface to the groundwater level is regarded as the non-liquefiable layer thickness H_1).

A pretest was performed in Step 3), and a number of similar field density tests were performed on the stabilized non-liquefiable layer. The results were averaged to measure the unit weight of the non-liquefiable layer. The results show that the total unit weight of the non-liquefiable layer was approximately 17.6 kN/□, and the relative density was estimated to be approximately 60%. Figure 6 shows the unit weight measurement test scene for the non-liquefiable layer. The volume of the sample was calculated by inserting a steel pipe into the composition ground and measuring the depth of the inserted steel pipe, and the unit weight was calculated by scooping up the soil to the bottom of the steel pipe and measuring its weight and water content. The non-liquefiable layer is in a very dense state, as shown in Fig. 6(b).

The unit weight of the liquefiable layer was considered to be the same as the unit weight estimated in Cases 1–4, and this was used for the analysis of the results.

3. Test Results And Analysis

3.1 Analysis of the Effect of the Embankment Height

3.1.1 Model Response

Figure 7 shows the time history of the input seismic load, response acceleration, excess pore water pressure, and settlement at the embankment crest based on the change in the embankment height. Particularly, Fig. 7(a) shows the test results for the horizontal ground section without embankment (H = 0 cm). Based on Figs. 1 and 7, A01 is the input acceleration time history measured on the shaking table, and A29, A27, A17, A23, and A21 are the response acceleration time histories at different positions of the input load (A01). In addition, A29 and A27 are the acceleration response time histories for each depth at an intermediate position between the embankment and the soil box wall (i.e., at a position that can be regarded as a free field). Moreover, A17 is the acceleration response time history directly below the embankment toe, and A23 and A21 are the acceleration response time histories for the depth at the center of the embankment. P57, P48, and P52 show the excess pore water pressure response time histories in the lower part of the free-field ground, embankment toe, and embankment center, respectively. In Case (a), D1 shows the settlement at the model central ground surface in the cross section without embankment. On the other hand, Cases (b)–(d) show the settlement at the center of the embankment crest.

In Fig. 7, in the case of H = 0 cm and H = 5 cm, the response of the acceleration in the ground below the embankment (A23, A21) did not respond after a certain time, which is similar to the acceleration response in the free field (A29, A27). This confirmed the occurrence of liquefaction. On the other hand, in the case of H = 10 cm and H = 15 cm, the response of the acceleration in the ground below the embankment continued although the magnitude decreased contrary to the response in the free field. The degree of liquefaction was confirmed to decrease. In the case of the accelerometer (A17) installed below the toe of the embankment, a peculiar response was observed (i.e., the measurement record was skewed in a certain direction with respect to the neutral axis), as shown in the figure. This phenomenon is caused by

the rotation of the accelerometer due to the lateral flow during excitation. This phenomenon becomes more severe as the lateral flow grows larger. In the cases of H = 10 cm and H = 15 cm, this phenomenon was found to enhanced and alleviated, respectively. Therefore, the degree of the lateral flow was found to be the largest when H = 10 cm.

In Fig. 7, the decrease in the degree of liquefaction in the ground below the embankment based on the increase in the embankment height can be confirmed not only in the above acceleration response but also in the response of the excess pore water pressure. This can be confirmed by the decrease in the excess pore water pressure ratio $\mathrm{r\_〖u〗}$, which is expressed as $\mathrm{r\_〖u〗} = \Delta \mathrm{u} \backslash / \sigma\_〖\mathrm{v0}〗'$. Here, $\Delta \mathrm{u}$ is the excess pore water pressure, and $\sigma\_〖\mathrm{v0}〗'$ is the initial vertical effective stress, as shown in P52. In the time traces of the pore water pressure in the figure, the initial vertical effective stress $\sigma\_〖\mathrm{v0}〗'$, which was roughly estimated at each location by using Eq. (1), is a reference stress used to determine how the soil is close to the zero-effective-stress state and is indicated by the dashed line.

$$\sigma_{vo}' = \sum \gamma' h$$

1

where γ' is the submerged unit weight of the sand ground, and h is the depth from the model surface.

Based on the response settlement (D1) at the embankment crest in Fig. 7, the embankment height and the embankment crest increased. However, the settlement in the case of H = 15 cm was slightly lower than that in the case of H = 10 cm. This is attributed to the mutually complex effects of the increase in the overburden pressure and the degree of liquefaction due to the increase in embankment height. In addition, it is assumed that there will be a specific embankment height where the settlement is the largest due to these two effects.

Figure 8 shows the distribution of the excess pore-water pressure ratio $r_u = u / \sigma'_{v0}$

after excitation based on the embankment height. In the case of a cross section without an embankment, the excess pore-water pressure ratio slightly increased from the center of the ground to the side, but the entire ground was liquefied without a significant difference ($r_u \geq 0.9$), as shown in Fig. 8(a). In Figs. 8(b)–(d), the excess pore-water pressure ratio in the lower part of the center of the embankment decreases as the embankment height increases, indicating a decrease in the degree of liquefaction. Compared to the case of H = 5 cm, the degree of liquefaction is slightly reduced in the case of H = 10 cm, but the difference between the excess pore-water pressure ratios in the free field and directly below the embankment is larger. The direction of the flux draws an arc from the lower part of the embankment toward the free field, and the change in the excess pore-water pressure ratio appears to be steep. This distribution characteristic indicates that the degree of lateral flow is greater. The lateral flow is smaller in the case of H = 15 cm than in the case of H = 10 cm if described in the same manner as above. From the result analysis, the complex effect of the embankment height on the degree of liquefaction and the degree of the lateral flow affecting the embankment settlement were determined.

3.1.2 Effect of the Embankment Height on the Settlement of the Embankment on Liquefiable Subsoil

The factors of the entire settlement of the embankment on the liquefiable ground should be related to the lateral flow, consolidation settlement of the subsoil, and settlement of the embankment (Towhata et al., 1999; Ohki et al., 2004). In this study, the embankment was constructed with gravel, and its density was increased to suppress the settlement as much as possible to exclude the settlement characteristics of the embankment and examine only the effect of the characteristics of the foundation ground on the embankment settlement. Consistent with this intention, the test results also showed that the settlement of the embankment was insignificant. Therefore, the total settlement was considered to be caused only by the lateral flow and consolidation settlement of the subsoil.

Figure 9 shows the effect of the embankment height on the amount of settlement caused by excitation at the crest of the embankment laid on the liquefiable sand ground. Figure 9(a) shows the settlement at the embankment crest based on the embankment height H, and Fig. 9(b) shows the ratio of the settlement of the embankment at different heights to the settlement of the horizontal ground without the embankment based on the ratio of the height of the embankment H to the height of the entire liquefiable layer HL.

Based on Fig. 9(a), the settlement increases as the embankment height increases, and it is constant or decreases above a certain height. The degree of liquefaction of the ground under the embankment decreases as the embankment height increases due to the overburden pressure, resulting in the decrease of the consolidation settlement due to liquefaction. This result is consistent with the test results presented above and those mentioned in a previous study (Prakash, 1981; Tabatabaei et al., 2019).

However, the lateral flow occurs because of the difference in the degree of liquefaction due to the location of the foundation ground, causing the embankment settlement to be greater than the decrease in the consolidation settlement. Therefore, the total settlement increased. Nevertheless, the degree of liquefaction in the soil layer near the surface decreases at all locations of the foundation ground when the embankment height is higher than a certain height, as shown in Figs. 8(c) and (d). Therefore, the embankment settlement by the lateral flow does not increase more than the decrease in the consolidation settlement based on the liquefaction degree. Therefore, the total settlement is constant or decreases. However, as this test result excludes the settlement of the embankment, in the case of an actual embankment, it is expected that the settlement due to deformation of the embankment based on the increase in the height of the embankment will increase. Contrary to the test results, there is a possibility that there is no decrease in the total settlement.

Based on Fig. 9(a), the settlement increases as the embankment height increases, and the settlement is constant or decreases above a certain height. Moreover, based on Fig. 9(b), compared to the settlement of the ground without the embankment, it is apparent that the embankment settlement due to liquefaction of the foundation increases with the embankment height. In addition, it increases up to two times when the embankment height is approximately 20% of the total liquefiable soil layer, and then it becomes

constant or decreases. A height equivalent to 20% may be considered rather low. However, considering that the width of the upper part of the railway embankment was generally 14 m and the slope of the embankment was 1:1.8, the width of the lower part of the embankment reached 28 m even if the embankment height was only 4 m. This result is reasonable to some extent because the width of 28 m at the bottom of the embankment can sufficiently reduce the degree of liquefaction and lateral flow by transmitting the overload of the embankment to the bottom, although the thickness of the liquefiable sand ground is approximately 20 m. This result shows an increase in the settlement by the embankment height with respect to the settlement of the liquefaction layer without embankment due to liquefaction. Moreover, it can be referred as a relative quantitative value rather than an absolute quantitative value. However, referring to the results of the previous study of Ha (2004), the settlement rate due to complete liquefaction of the liquefaction ground without dikes was within 5% of the total liquefied ground. Based on the above results, in a conservative way, the settlement of the embankment on the liquefiable foundation can be predicted to be approximately 10%, which is twice the 5%.

For example, the maximum settlement due to ground liquefaction of the embankment placed on the liquefied ground and the embankment height showing the maximum settlement can be estimated if the thickness of the entire liquefaction layer is 20 m. On the other hand, the embankment height of 4m, which is 20% of the total liquefiable layer thickness 20 m, shows the maximum settlement. For an embankment with a height of 2 m, which is 10% of the total liquefaction layer thickness of 20 m, it can be presented as a reference value of the maximum value of the embankment settlement due to the liquefaction from a conservative point of view.

3.2 Analysis of the Effect of the Non-liquefiable Layer Thickness

3.2.1 Model Response

Figure 10 shows the time history of the input seismic load, response acceleration, excess pore water pressure, and settlement at the embankment crest for the shaking table test in which the non-liquefiable layer thickness was changed to 0, 4.5, 10.5, and 13.5 cm for the embankment with a constant height of 10 cm. The instrument number is the same to the one described in Fig. 7.

In Fig. 10, in all cases except Case 7, liquefaction occurred in the free field because the response of the acceleration (A29, A27) did not occur after a specific time. On the other hand, the response of the acceleration in the ground below the embankment continued although the magnitude decreased. It can be confirmed that the degree of liquefaction decreased or liquefaction did not occur. In Case 7, liquefaction did not occur because the magnitude of the response acceleration did not change significantly in the free field or under the embankment. In all cases except for Case 7, the measurement record of the accelerometer (A17) installed just below the toe of the embankment is skewed in a certain direction with respect to the neutral axis. The degree of skewing indirectly indicated the degree of lateral

flow. The degree of skewing decreased as H1 increased. This phenomenon did not appear in Case 7, in which H1 is the largest.

In Fig. 7, the decrease in the degree of liquefaction in the ground below the embankment based on the increase in the non-liquefiable layer thickness can be confirmed by the above acceleration response and the response of the excess pore water pressure. The excess pore-water pressure ratio r_u decreases, as shown in P52. In particular, this value sharply decreased in Case 7, where H1 = 13.5 cm.

The settlement at the embankment crest decreased as the non-liquefiable layer thickness increased based on the response settlement (D1) at the embankment crest in Fig. 10. In Case 7, the settlement rapidly decreased and was almost insignificant. That is, the increase in the non-liquefiable layer thickness suppresses the lateral flow near the ground surface affected by the embankment weight and reduces the degree of liquefaction of the underlying ground. Therefore, the embankment settlement is reduced, and the occurrence of liquefaction of the entire subsoil is prevented when it reaches a certain thickness (H1 = 13.5 cm in this test), resulting in the settlement reaching an insignificant level.

Figure 11 shows the distribution of the excess pore-water pressure ratio $\mathrm{r}_u = u/\sigma'_{v0}$ excitation based on the non-liquefiable layer thickness for the embankment with a constant height of 10 cm. In Case 3 shown in Fig. 11(a), the difference between the excess pore-water pressure ratios in the free field and directly below the embankment is larger. The direction of the flux draws an arc from the lower part of the embankment toward the free field, and the change in the excess pore-water pressure ratio appears to be steep. This distribution characteristic indicates that the degree of lateral flow is greater. The degree of such lateral flow decreases as the non-liquefiable layer thickness increases, as shown in Figs. 11(b) and (c). In this study, the lateral flow did not occur at the thickness of 13.5 cm shown in Fig. 11(d), and the excess pore-water pressure ratio in the ground rapidly decreased. Therefore, liquefaction of the foundation ground did not occur. The increase in the thickness of the non-liquefiable layer under the embankment reduces the settlement by suppressing the lateral flow and decreasing the degree of liquefaction by increasing the resistance to liquefaction of the entire foundation ground.

Therefore, this reduces the embankment settlement. It is expected that there will be a certain non-liquefiable layer thickness in which this settlement can be rapidly reduced.

3.2.2 Effect of the Non-liquefiable Layer Thickness on the Settlement of the Embankment on the Liquefiable Subsoil

Figure 12 shows the effect of the non-liquefiable layer thickness on the settlement caused by excitation at the crest of the embankment laid on the liquefiable sand ground. In addition, Fig. 12(a) shows the ratio of the settlement SH_1 of the embankment with different non-liquefiable layer thicknesses H_1 to the settlement $SH_{1=0}$ of the horizontal ground without embankment based on the ratio of H1 to the embankment height H. Moreover, Fig. 12(b) shows $SH_1/SH_{1=0}$ based on the ratio of H1 to the height of the entire liquefiable layer thickness HL.

SH1/SH1 = 0 decreases in the form of a quadratic function when the embankment is placed on the ground with a large non-liquefiable layer thickness, as shown in Fig. 12(a). The settlement was reduced by approximately 20% compared to the settlement of the embankment placed on the ground with H_1 = 0 if the non-liquefiable layer thickness was approximately 50% of the embankment height. In addition, limited to the results of this test, the embankment settlement was almost insignificant when the non-liquefiable thickness layer was approximately 1.4 times the embankment height. This is because the degree of liquefaction of the subsoil under the embankment decreases when the embankment height increases due to the effect of the overburden load of the embankment. In addition, the lateral flow of the superficial liquefaction layer, which easily causes a lateral flow, is suppressed when the non-liquefiable layer thickness increases.

Figure 12(b) shows $SH_1/SH_{1=0}$ based on the ratio of H_1 (= 0, 4.5, 10.5, and 13.5 cm) to the height of the entire liquefiable layer thickness H_L (= 50 cm). For reference, considering that the scale factor of the model in this test is 1/40, H_L=50 cm can be considered to correspond to 20 m in the actual ground. Based on Fig. 12(b), the embankment settlement decreases as the non-liquefiable layer thickness increases. In addition, the settlement reaches a negligible level when H1 reaches approximately 30% of H_L because liquefaction hardly occurs in the free field and the lower part of the embankment. Note that the results of Fig. 12(a) are effective up to an H_1/H_L value of approximately 0.3, and the settlement above that is almost insignificant. A previous study (MLIT, 2013) suggested that damage caused by liquefaction to buildings placed on easily liquefiable ground is almost impossible to occur when the non-liquefiable layer thickness exceeds 5 m, regardless of the LPI representing the degree of liquefaction. In this study, a scale factor of 1/40 was applied. In the model, the depth of the entire liquefaction layer of 50 cm corresponds to 20 m in the actual ground, and the non-liquefiable layer thickness satisfying H_1/H_L = 0.3 corresponds to 6 m. Based on the results of this test, the settlement due to liquefaction hardly occurs when the non-liquefiable layer thickness of the embankment foundation is 6 m or more, which is the limit value. Therefore, the results of this test can be considered to be consistent with the results of previous studies.

4. Conclusion

In this study, 1-g shaking table tests were performed on a total of seven cases under various test conditions (i.e., the embankment height and the non-liquefiable layer thickness below the embankment were changed for the same input seismic load conditions). During the test, accelerometers, pore water pressure transducers, and LVDTs were embedded inside the foundation ground or installed on the surface of the embankment to measure its responses to shaking. The main conclusions drawn from the analysis of the experimental results are as follows.

1. The procedure and method of an intuitive 1-g shaking table model test for analyzing the behavior of a two-dimensional embankment-ground system based on the stratum composition changes, such as changes in the height of the embankment and the non-liquefiable layer thickness of the ground under the embankment, were presented. In addition, we presented well-documented experimental data

necessary to understand the settlement behavior because of the two-dimensional interaction between the embankment and the subsoil.

2. The degree of liquefaction of the ground under the embankment decreases as the embankment height increases due to the overburden pressure. Therefore, the consolidation settlement due to liquefaction decreases. However, a lateral flow occurs due to the difference in the degree of liquefaction by the location of the foundation ground, causing the embankment settlement to be greater than the decrease in the consolidation settlement. Therefore, the total settlement increased. Nevertheless, the degree of liquefaction in the soil layer near the surface decreases in all locations of the foundation ground when the embankment height is higher than a certain height, as shown in Figs. 8(c) and (d). The embankment settlement by the lateral flow does not increase more than the decrease in the consolidation settlement based on the liquefaction degree. Moreover, the total settlement is constant or decreases. Compared to the settlement of the ground without embankment, it is apparent that the embankment settlement due to liquefaction of the foundation increases with the embankment height compared to the settlement of the ground without embankment. Particularly, it increases up to two times when the embankment height is approximately 20% of the total liquefiable soil layer. Therefore, it is constant or decreases. Based on the test results, previous research results, and the assumption that the settlement of the embankment itself is insignificant, the reference value for the maximum embankment settlement was proposed as 2 m due to liquefaction of the foundation subsoil at the actual site.
3. The increase in the thickness of the non-liquefiable layer under the embankment reduces the settlement by suppressing the lateral flow and decreasing the degree of liquefaction by increasing the resistance to liquefaction of the entire foundation ground, resulting in the reduction of the embankment settlement. The ratio of the settlement of the embankment with different non-liquefiable layer thicknesses to the settlement of the horizontal ground without embankment decreases in the form of a quadratic function since the embankment was placed on the ground with a large non-liquefiable layer thickness. The settlement was reduced by more than 20% compared to the settlement of the embankment placed on the ground with $H_1 = 0$ if the non-liquefiable layer thickness was approximately 50% of the embankment height. In addition, limited to the results of this test, the embankment settlement was almost insignificant when the non-liquefiable thickness layer was approximately 1.4 times the embankment height. Based on the test results, previous research results, and the assumption that the settlement of the embankment itself is insignificant, 6 m was proposed as the reference value for the minimum non-liquefiable layer thickness that can be judged to be insignificant in the embankment settlement due to liquefaction of the foundation subsoil at the actual site.

Declarations

Acknowledgement

This study was supported by the Korea Agency for Infrastructure Technology Advancement (KAIA) grant funded by the Ministry of Land, Infrastructure, and Transport (Grant 21SCIP-C155167-03:MT21027).

References

1. Ha, I. S. (2004). Evaluation of post-liquefaction behavior of saturated sand deposits using shaking table tests. Ph.D. thesis, Department of Civil Engineering, Seoul National University, Seoul.
2. Ishihara, K., &Yoshimine, M. (1992). Evaluation of settlements in sand deposits following liquefaction during earthquakes. Soils and Foundations, 32(1), 173–188.
3. Iwasaki, T. (1986). Soil liquefaction studies in Japan: State-of-the-art. Soil Dynamics and Earthquake Engineering, Vol. 5(1), 2–68.
4. Iwasaki, T., Tatsuoka, F., Tokida, K., and Yasuda, S. (1978). A practical method for assessing soil liquefaction potential based on case studies at various sites in Japan. Proceedings of the 2nd International Conference on Microzonation, San Francisco, 885–896.
5. Koga, Y. and Matsuo, O. (1990). Shaking table tests of embankments resting on liquefiable sandy ground. Soils and Foundations, 30(4), 162–174.
6. Matsuo, O. (1996). Damage to river dikes. Soils and Foundations, 36(1), 235–240.
7. Ministry of Land, Infrastructure and Transport and Tourism (MLIT). (2013) Technical Guideline for Evaluation of Liquefaction Damage Potential on Housing Sites (in Japanese).
8. Nozawa, S., Shirasaki, H., Wada, A., and Tomori, M. (2019). Damage and restoration of the railway structures caused by the 2011 off the Pacific coast of Tohoku Earthquake. Journal of Geotechnical Engineering, 7(1), 127–137 (in Japanese).
9. Ohki, M., Sawada, Y., Kanaguchi, Y., and Moroku, A. (2004). Experimental study of model embankment of liquefaction ground. 13th World Conference on Earthquake Engineering, Vancouver, Paper No. 809.
10. Ohki, M., Seki, M., Nagao, T., and Nakano, M. (2013). Experiment valiation of five failure modes and the proposal of seismic reinforcement in the railway embankment. Journal of Civil Engineering, 69(2), 174–185 (in Japanese).
11. Park, Y. H., Kim, S. R., Kim, S. W., and Kim, M. M (2000). Liquefaction of embankment on sandy soils and the optimum countermeasure against the liquefaction. 12th World Conference on Earthquake Engineering, Auckland, Paper No. 1170.
12. Prakash, S. (1981). Soil Dynamics, McGraw-Hill Book Company, New York.
13. Sasaki, Y. and Matsuo, O. (1983). Shaking table tests on the remedial measures to improve seismic stability of embankments. Proceedings of 15th UJNR Joint Meeting, Tsukuba, PWRI.
14. Sawada, R., Miroku, A., Ohki, M., Kanaguchi, Y., Teshigawara, A., and Tateyama, M. (2003). Experimental studies of model embankments on liquefaction ground (Part 1,2). Japan National Conference Geotechnical Engineering, 2, 1315–1318 (in Japanese).

15. Tabatabaei, S. A., Esmaeili, M, and Sadeghi, J. (2019). Investigation of the Optimum Height of Railway Embankments during Earthquake Based on Their Stability in Liquefaction. Journal of Earthquake Engineering, 23(5), 882–908.
16. Tokimatsu, K., & Seed, H. B. (1987). Evaluation of settlements in sands due to earthquake shaking. Journal of Geotechnical Engineering, 113(8), 861–878.
17. Towhata, I., Orense, R. P., and Toyota, H. (1999). Mathematical principles in prediction of lateral ground displacement induced by seismic liquefaction. Soils and Foundations, 32(3),73–90.

Tables

Table 1.

Index properties of the silica sand used for the model ground composition

Parameter	Value
Specific gravity, G_【s】	2.65
Maximum dry density, ρ_【d, max】(g/㎤)	1.85
Minimum dry density, ρ_【d, min】(g/㎤)	1.37
Mean particle size, D_【50】(mm)	0.11
Uniformity coefficient, C_【u】	2.89
Coefficient of curvature, C_【c】	1.07
Permeability, k (m/sec)	2.51×10-4

Figures

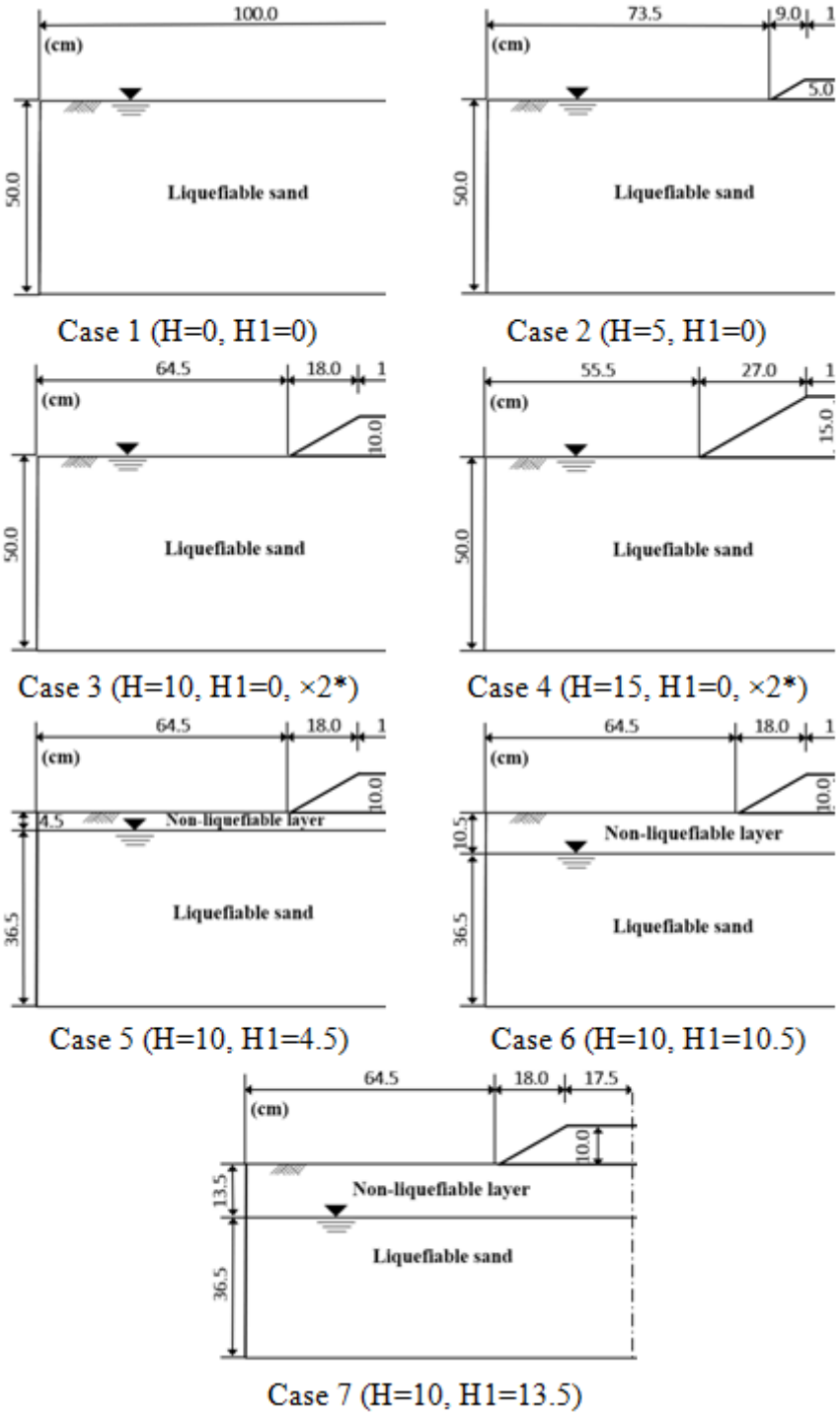

Figure 1

Schematic of each test setup. H is the embankment height, and H1 is the non-liquefiable layer thickness; *×2 means that two tests were conducted under the same conditions.

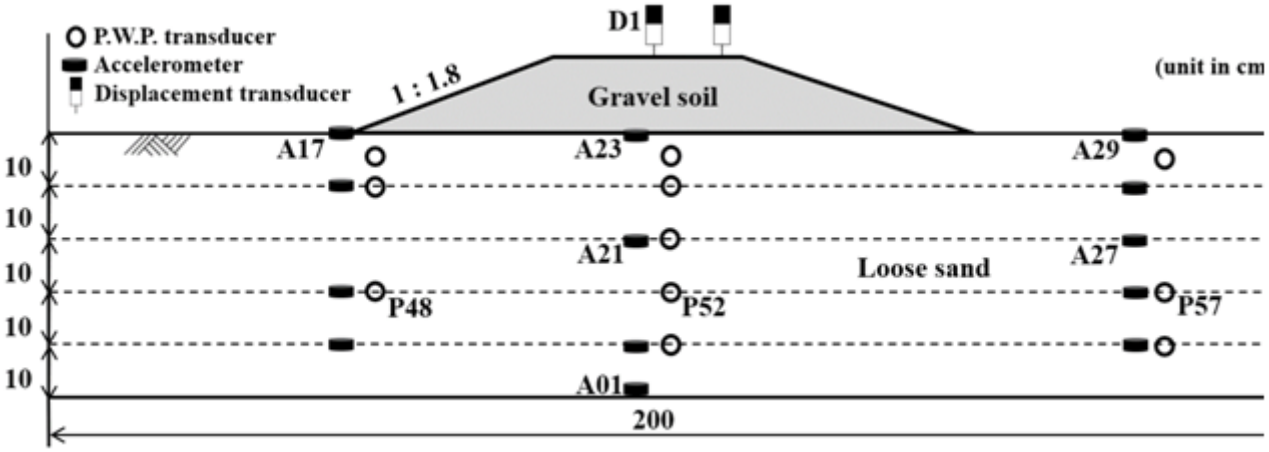

Figure 2

Instrument layout

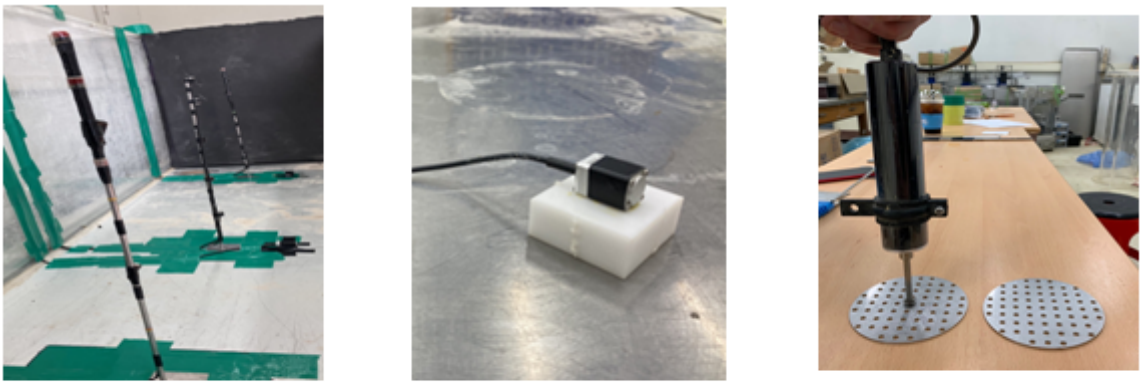

(a) P.W.P. transducer

(b) accelerometer

(c) LVDTs

Figure 3

Installation method of each measuring sensor

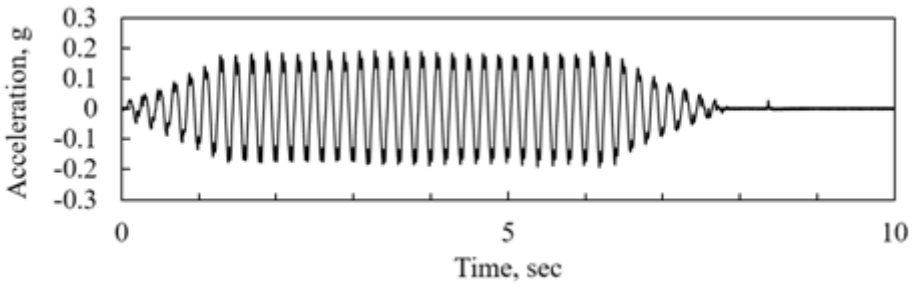

Figure 4

Input acceleration time history

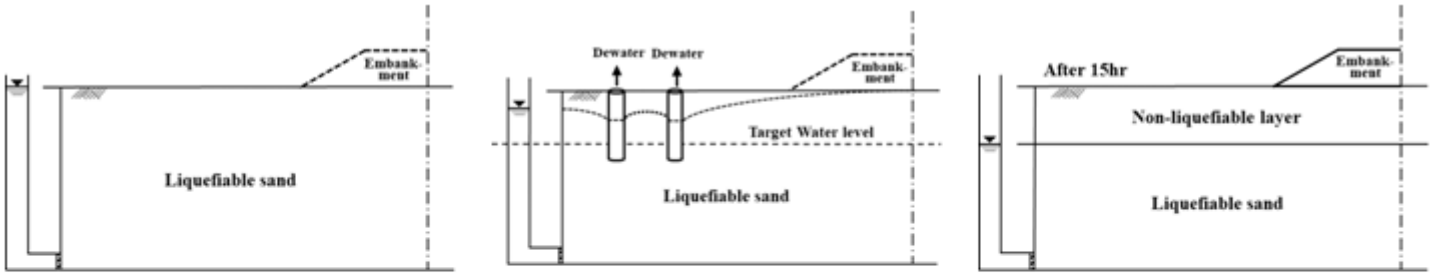

(a) Composition of liquefiable sand ground

(b) Composition of the upper non-liquefiable layer by dewatering

(c) Stabilization after embankment installation

Figure 5

Schematic of the composition procedure of test cross-sections

(Cases 5, 6, and 7) with the non-liquefiable layer

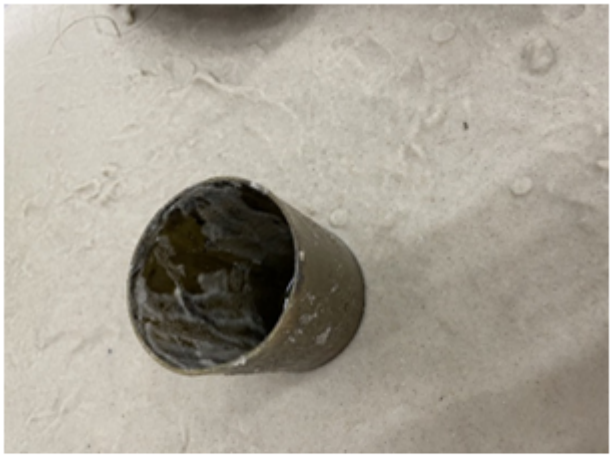

(a) Pipe insertion and volume measurement

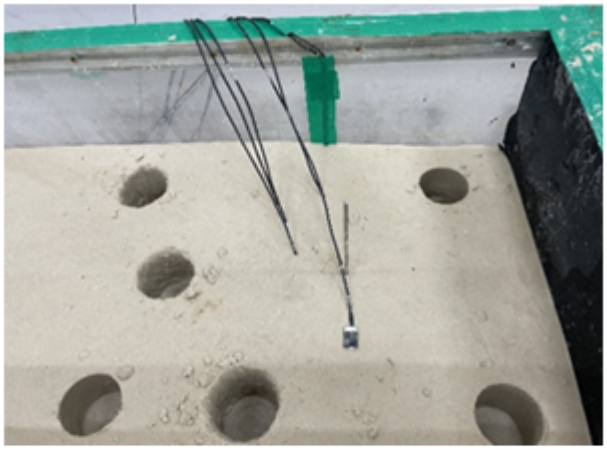

(b) Sampling and density test

Figure 6

Density measurement of the non-liquefiable layer

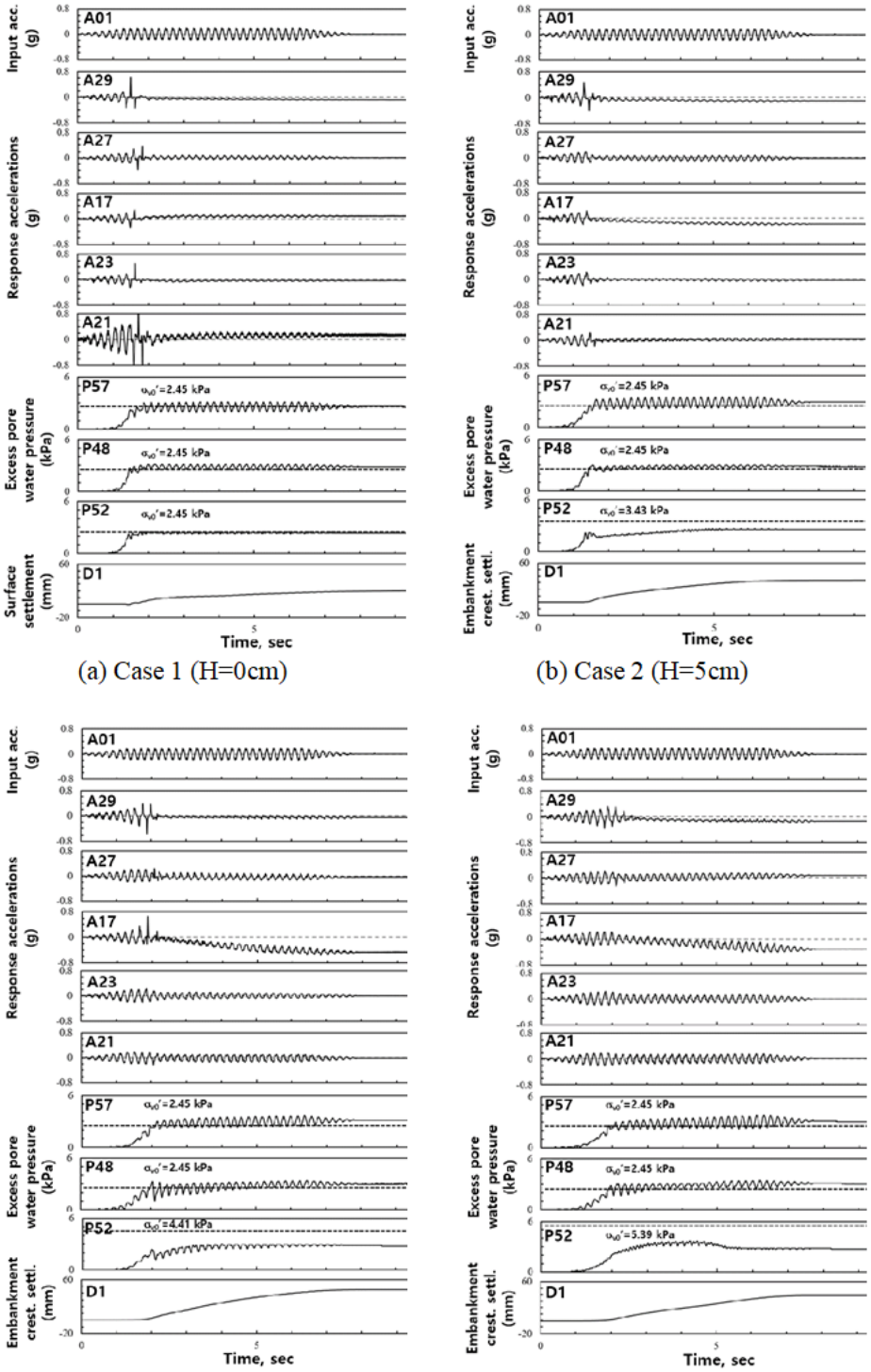

Figure 7

Time histories of input and response accelerations, excess pore water pressures, and crest settlement with embankment height H (surface settlement in Case (a))

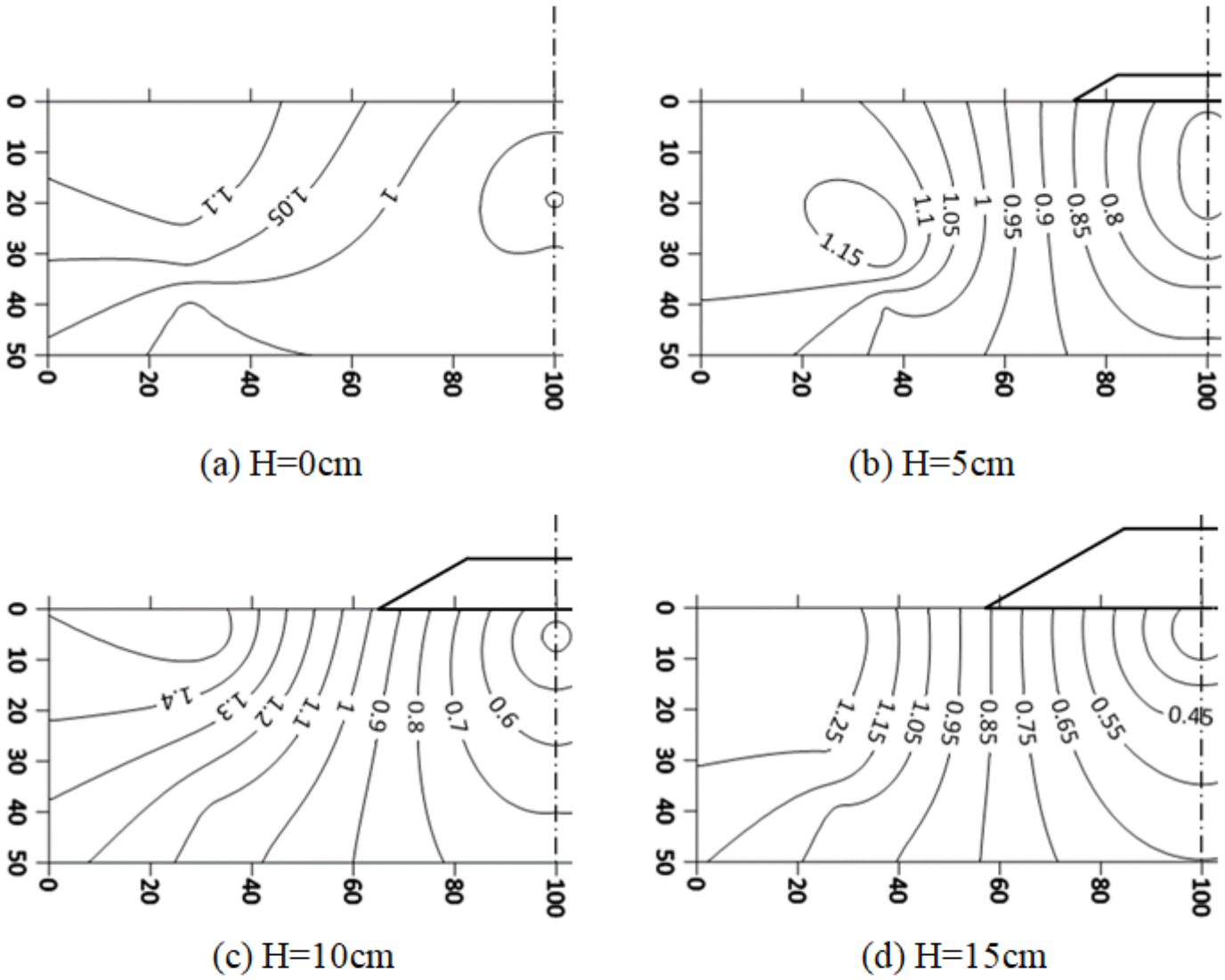

Fig. 8. Contour of excess pore-water pressure ratio r_〖u〗 = Δu\/σ'_〖v0〗 after shaking with embankment height H

Figure 8

See image above for figure legend.

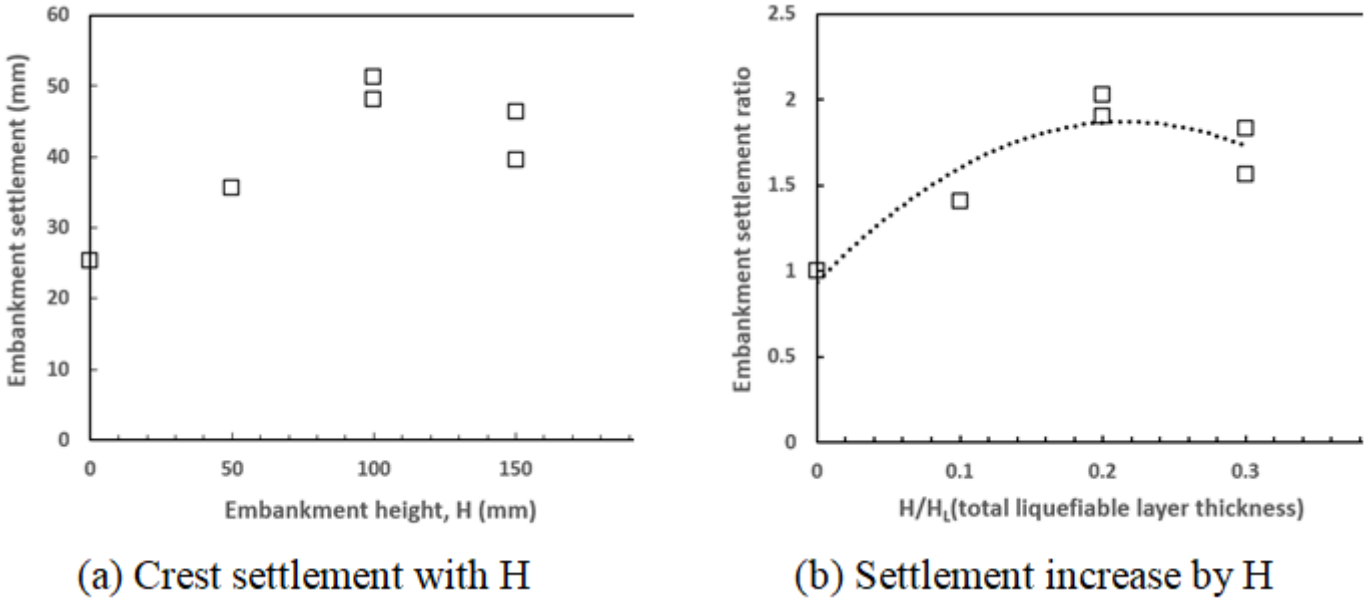

Figure 9

Effect of the embankment height on the settlement of the crest of embankments on the liquefiable sand ground

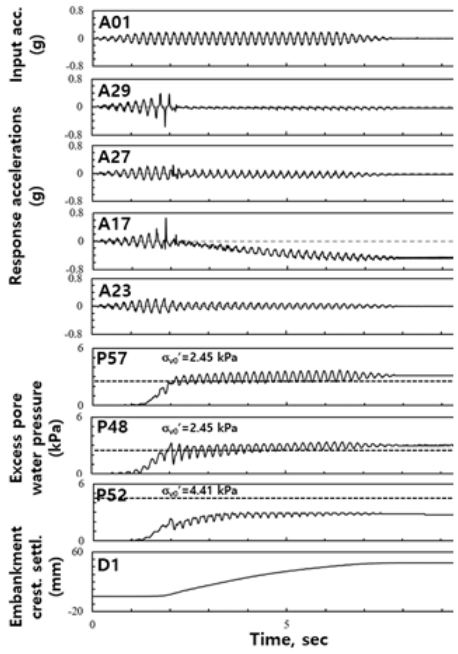

(a) Case 3 (H=10cm, H1=0cm)

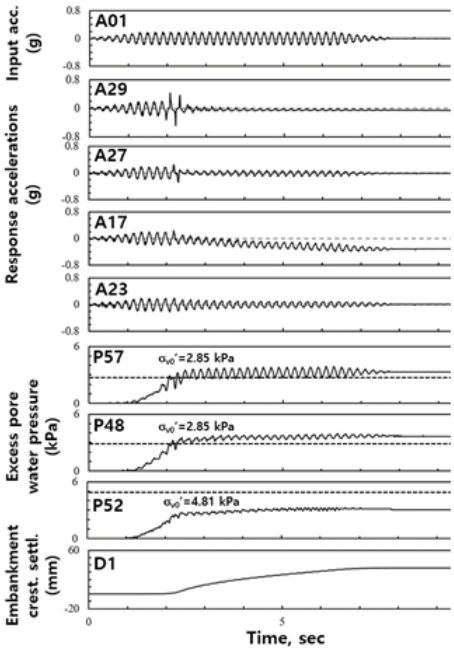

(b) Case 5 (H=10cm, H1=4.5cm)

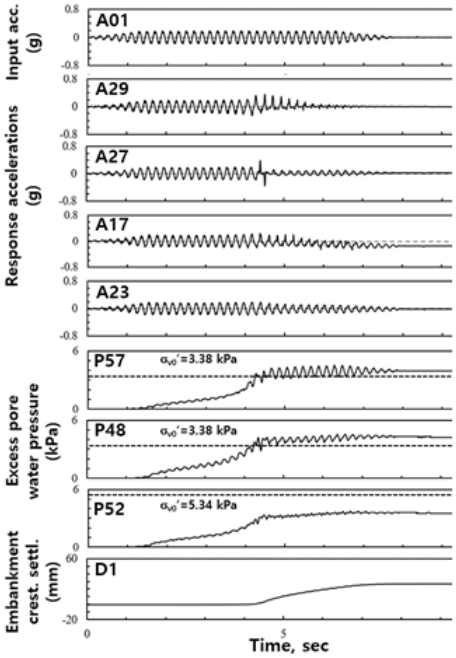

(c) Case 6 (H=10cm, H1=10.5cm)

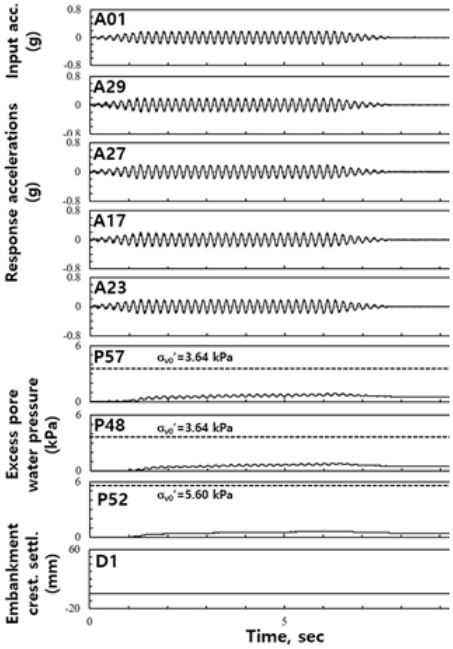

(d) Case 7 (H=10cm, H1=13.5cm)

Figure 10

Time histories of the input and response accelerations, excess pore water pressures, and crest settlement with non-liquefiable layer thickness H1

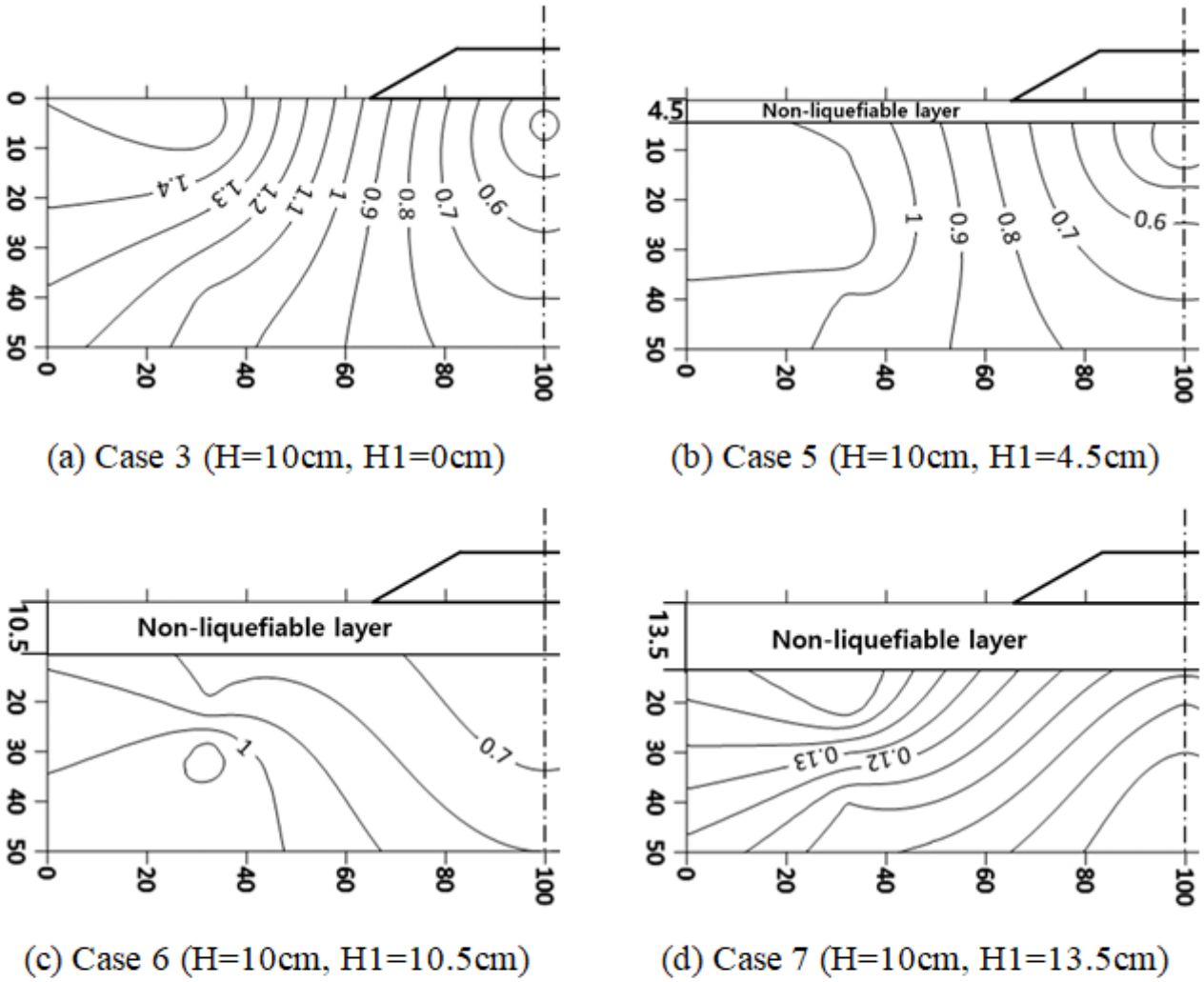

(a) Case 3 (H=10cm, H1=0cm)

(b) Case 5 (H=10cm, H1=4.5cm)

(c) Case 6 (H=10cm, H1=10.5cm)

(d) Case 7 (H=10cm, H1=13.5cm)

Fig. 11. Contour of the excess pore-water pressure ratio r_〖u〗 = u\/σ′_〖v0〗 after shaking, where H1 is the non-liquefiable layer thickness, and H is the embankment height

Figure 11

See image above for figure legend.

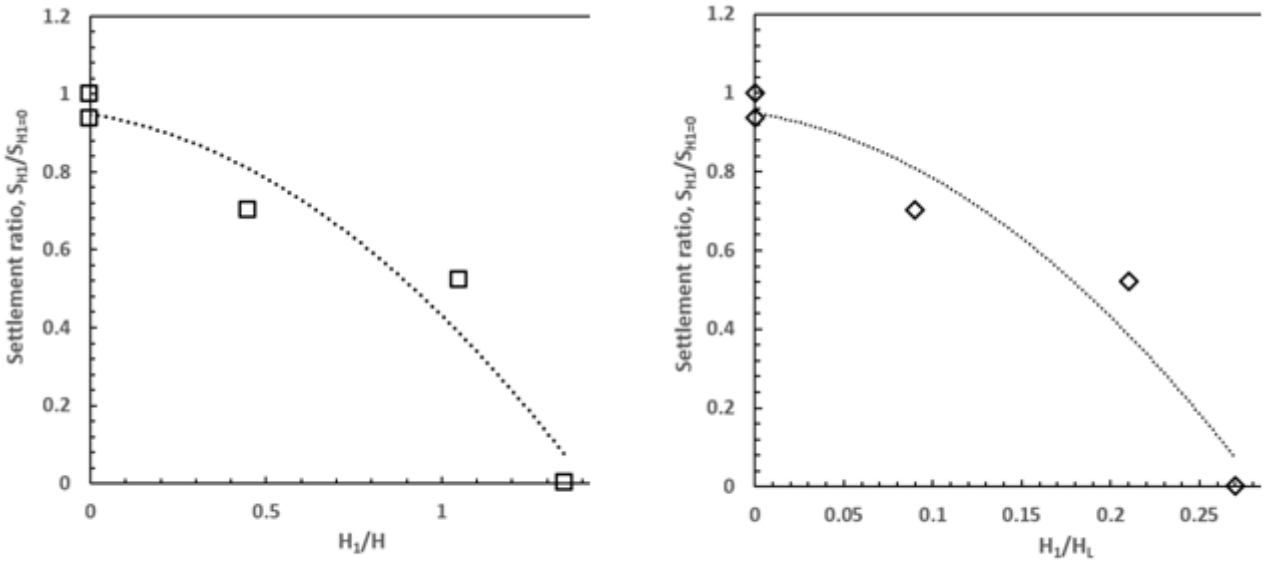

(a) Embankment settlement with H1/H

(b) Embankment settlement with H1/HL

Figure 12

Effect of the non-liquefiable layer thickness on the settlement of the crest of embankments on the liquefiable sand ground